PRELIMINARY RESULTS OF THE CRYSTAL COLLIMATION TEST IN UA9

D. Mirarchi*, G. Cavoto, INFN Roma and Univ. Roma Sapienza, Roma, Italy

R. Losito, W. Scandale, CERN, Geneva, Switzerland

A. Taratin, JINR, Dubna, Russia

for the UA9 collaboration.

Abstract

We present a detailed analysis of the beam loss data collected at the SPS during the 2009 machine developments devoted to test crystal collimation. Scintillator counters and GEM detectors were installed in special points to detect the effect of inelastic interaction of protons with the crystals in various orientation with respect to the beam. Clear correlations of the counting rates with the crystal positions and orientation were detected during the data-taking and were crucial to put the crystal in optimal channeling position. For one of the crystal the pattern of losses showed evidence of several planar and axial channeling conditions.

INTRODUCTION

The UA9 experiment is located in the SPS straight section LSS5 with the aim of investigating the feasibility of beam collimation with bent crystals. The peculiar features of charged particles interaction with the ordered structure of a crystal [1] can be exploited. Different regimes are in fact possible depending on the relative orientation of particle direction and crystal symmetry axes or planes: multiple scattering when a random orientation is chosen, axial channeling when particles are parallel to a line of atoms, volume reflection (VR) when the particles reverse their transverse momentum hitting the lattice planes, or the planar channeling - preferred in this experiment - when the particles are trapped between the lattice planes largely decreasing their interaction with the material. If the lattice planes are mechanically bent the channeled particles are deflected. Such configuration can be used as a primary collimator for a circulating beam instead of a more traditional passive scatterer [2].

APPARATUS

The complete layout of the UA9 apparatus is described in details elsewhere [3]. For this paper some detectors positioned in relevant locations are used, in particular radiators of scintillation and Cherenkov light readout by photomultipliers (PMT) and Gas Electron Multiplier (GEM) [4] detectors.

Scintillators (TEC3 and TEC4) are located with a GEM detector (GEM2) immediately after a tank containing two bent Si crystals. A second GEM detector (GEM1) is installed immediately before the tank and used only to check the level of background. Another pair of scintillator

(QD1 and QD2) is installed between the first and second quadrupole following the straight section. Each scintillator has a $10x10 \, cm^2$ active surface while the GEM detector counts particles crossing an anode segmented in 16x8 6x12 mm^2 pads. They are all installed outside the beam pipe at a lateral distance of about 10 cm and therefore they are sensitive to the secondary products of inelastic interaction of beam particles. A quartz Cherenkov radiator, on the contrary, is located inside the beam pipe and attached after a tungsten absorber along the deflected beam direction. Its PMT signal rate (TACW1) should be directly proportional to the number of protons crossing the radiator.

ALIGNMENT TO THE BEAM

A procedure to find the orbit of the circulating beam during the data-taking operation was defined to establish the relative positions of the various movable devices of the apparatus. A LHC-type collimator [5] is used to initially determine the orbit position: from their rest positions (maximal aperture) the two jaws are independently moved towards the beam. When the beam is reached, a sudden increase of the secondary radiation is detected by the nearby beam loss monitors: the collimator is therefore left in such position to remove particles from the external portion of the beam. After this all the other devices are aligned: each object is moved initially with few mm steps and then reducing them down to fraction of mm when the alignment position is approached. Until the object stays in the shadow of the LHC-type collimator the beam loss rate does not change, but as soon as it goes past the collimator it touches the circulating beam and an increase of the radiation in the region close to such device is detected.

Figure 1: Lateral position of crystal 1 (black solid) and rate measured by TEC3 located immediately after the tank (red dashed) as a function of the acquisition time.

01 Circular Colliders

T19 Collimation and Targetry

An example of this procedure is shown in Fig.1. It is evident that until 15:34 while varying the crystal position, the rate measured by TEC3 stays constant. At 15:34 a first peak in the radiation losses is detected and then other five peaks are seen corresponding to the following five steps of the motion of the crystal. The higher rates demonstrate that the crystal is entering a deeper region of the beam. The position of the first peak of the radiation loss is chosen as alignment position relative to the LHC-type collimator. All the other devices are aligned in this way. After that the two jaws of the LHC-type collimator are opened to their rest position.

WORKING POINT AND OFF-LINE ANALYSIS

The UA9 detectors considered in this paper are especially useful to find the optimal working point of the bent crystal as shown in Fig.2. A scan of the angular position of the crystal is made and the rate measured by the detectors recorded. The occurrence of several planar channeling regimes due to the presence of secondary lattice symmetry planes is visible. Volume reflection regime is also seen for angular position close to the channeling peaks. The optimal point is chosen as the position with the largest decrease of measured radiation losses, in this case around -2000 μrad.
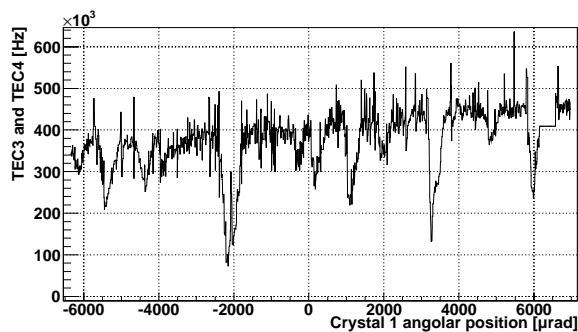
Figure 2: TEC3 and TEC4 coincidence rate as a function of the crystal 1 angular position. Several minima corresponding to different symmetry planes where crystal channeling is active are clearly seen. GEM2 detector (not shown in figure) shows the same pattern. The sudden increase of the rates are due to instabilities of the beam orbit that were present during that particular day of dataking and not correlated to the presence of the crystal.

The pattern shown in Fig.2 was successfully reproduced by a simulation based on the model given in [6]. In Fig.3 we show the comparison of the simulation (denoted with 2 in Fig.3) with the measured dependence of scintillators count (denoted with 1 in Fig.3) on the angular position of the crystal 1 during the scan with the goniometer around a specific channeling position. The flat dot-dashed line in Fig. 3 shows the count level for the orientations when the

crystal acts as an amorphous substance (amorphous orientations). The number of particle passages through the crystal before they either reach the tungsten absorber aperture or are lost due to inelastic interactions is determined by the angular kick values due to multiple Coulomb scattering in the crystal. A minimum at the goniometer angle around -1700μrad appears since a larger part of the beam halo particles are deflected by the crystal in channeling states, therefore avoiding inelastic interactions in the crystal. The beam losses decrease by a factor five with respect to the amorphous orientation. Furthermore, a wider area of beam loss reduction is present at position larger than -1700 μrad due to VR of halo particles: the angular kick due to VR is θ_{vr}=22 μrad whereas the RMS multiple scattering angle is θ_{ms}=10 μrad. Therefore, particles pass through the crystal before being absorbed fewer times than in the amorphous orientations. This reduces their inelastic interaction losses in the crystal. There is a second minimum in the theoretical dependence, which is at the angular distance from the main minimum of about the crystal bending angle (150 μrad). In this case, the whole VR region of the crystal is on the same side relative to the beam envelope direction. Therefore, particles acquires angular kicks of one polarity due to VR and more quickly reach the tungsten absorber. The experimental scan does not entirely reproduced such features: this can be caused by the crystal torsion (different orientations of the crystal planes along a vertical direction), so that the different vertical parts of the crystal deflect halo particles in a different way. Moreover, the instability of the goniometer or of the circulating beam can also smooth such dependence.
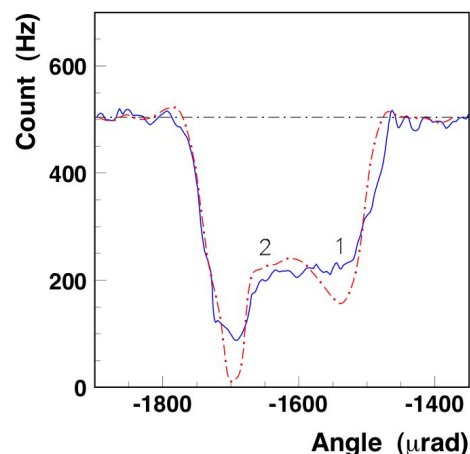
Figure 3: Comparison of angular scan simulation (red) with data (blue line). Flat dot-dashed line is the prediction for an amorphous orientation.

Another fundamental use of such detectors is the offline validation of the operations made during the data-taking. An example is show in Fig.4 and 5 where the comparison

between the measured rates and position of right LHC-type collimator jaw position is shown. Such jaw is on the side of the crystal deflected beam. A scan of the collimator jaw position is made with the crystal at the channeling angular point. The tungsten absorber is left in a location to fully intercept the crystal extracted beam. The collimator jaw is then increasingly closed. We expect that in the region close to the crystal the radiation losses (seen by TEC3) are constant during the whole scan. In the region nearby the collimator (that is after the crystal region) we expect to see an increase of the measured lossed (QD2) as soon as the crystal extracted beam is touched by the jaw. When the extracted beam is completely intercepted by the jaw the QD2 rate should become constant. At the same time a decrease in the rate of the Cherenkov detector on the absorber (TACW1) located after the collimator region should be observed since the deflected protons should be increasingly absorbed by the collimator. This is clearly seen in Fig.4.
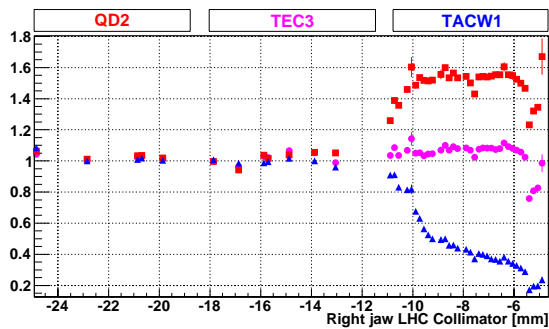
Figure 4: QD2 (red square), TEC3 (purple dot) and TACW1 (blue triangle) relative rates as a function of the right LHC-type collimator position with crystal in channeling position. For each detector its rates is given normalized to its rate measured in a reference position around -18 mm.

On the contrary for another collimator scan shown in Fig.5 a different configuration is observed. As soon as the collimator jaw goes beyond the -8 mm position it becomes the primary collimator, as can be inferred by the decreasing rate of TEC3. The particles that should impinge on the crystal are instead absorbed by the collimator jaw. This situation is unwanted since the crystal should be the primary collimator whenever its collimation properties are studied. Another interesting observation is related to the TACW1 rate. It never goes to zero even when the collimator jaw is in a position to fully intercept the extracted beam. This can be due to the fact that the LHC-type collimator does not have 100% efficiency to absorbe the protons, a fact that should be taken into account in the experiment simulation.

CONCLUSIONS

UA9 scintillator, GEM and Cherenkov detectors are a key component for the experiment operation and the analysis of data to study beam collimation with crystal channeling. Relative positions of the various movable devices
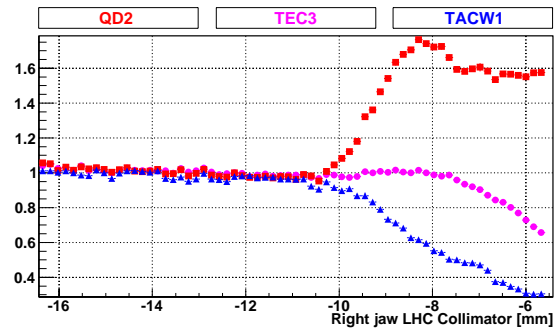
Figure 5: QD2 (red square), TEC3 (purple dot) and TACW1 (blue triangle) relative rates as a function of the right LHC-type collimator position with crystal in channeling position. For each detector its rate is given normalized to its rate measured in a reference position around -14 mm.

of the apparatus are determined using the rates measures by those detectors. This allows to determine the deflection angle of the channeled beam and to provide crucial inputs to the simulation for the determination of collimation efficiency. Last but not least, such detectors are the basic devices to find the optimal crystal working point during operation in collimation mode.

REFERENCES

[1] V.M. Biryukov, Y.A. Chesnokov, V.I. Kotov. Crystal channeling and its application at high energy accelerators: Springer, 1996.

[2] R. Assmann et al, "Designing and Building a Collimation System for the High-Intensity LHC Beam", in PAC03 proceedings.

[3] R.Losito, "UA9 Instrumentation and Detectors in the CERN-SPS", these proceedings.

[4] G.Bencivenni et al. Nucl.Instrum.Meth.A488:493-502,2002.

[5] UA9 MD report of 13-14 July 2009.

[6] A.M. Taratin and S. A. Vorobiev, Sov. Phys. Tech. Phys.30, 927 (1985).